

HIGH-FIDELITY LINEAR FRACTIONAL REPRESENTATION OF THE BENDING MODES OF A LAUNCH VEHICLE

Mirko Aveta⁽¹⁾, Patrizia Cotugno⁽¹⁾, Alessandro Lopez⁽¹⁾, Giuseppe Leto⁽¹⁾, Gianluca Curti⁽²⁾

⁽¹⁾AVIO, mirko.aveta@avio.com

⁽¹⁾AVIO, patrizia.cotugno@avio.com

⁽¹⁾AVIO, alessandro.lopez@avio.com

⁽¹⁾AVIO, giuseppe.letto@avio.com

⁽²⁾ESA-ESRIN, Gianluca.Curti@ext.esa.int

ABSTRACT

This work presents the design and application of a high-fidelity linear fractional representation (LFR) of the bending modes of a multi-stage launch vehicle. Such LFR allows to reconstruct from the mass and stiffness of each structural component the modal eigenfrequencies, deflections and rotations. The proposed LFR manages to duplicate within a generalized state space model of the launcher what would otherwise be only an outcome of a Monte Carlo (MC) analysis carried out with a Finite Element Model (FEM). As a consequence a robust design of the bending filters can now be carried out with further understanding of the flexibility of the launcher at system level. With this methodology, a worst case analysis can now provide worst case perturbations directly considering the stiffness budget parameters. It is also possible to predict the impact of any stiffness budget variation on stability. This further insight allows to include payload variability in the definition of such LFR. Ultimately, enabling: (1) the definition of generic LFRs for a launch vehicle; (2) the possibility to provide an *availability* certificate on the control law that allows to assess its robustness to last minute changes; (3) the design of robust control laws exploiting such *availability metric*. Results are presented taking VEGA-E as a benchmark.

1 INTRODUCTION

Today, there is an ever growing and competing satellite transportation market, featuring a large variety of satellite transportation solutions that include small launchers, piggyback systems, space tugs, air-lifted systems, etc. In this context, a crucial aspect for the deployment of a competitive expendable launch vehicle is to make its recurrent GNC tuning effortless. Ideally, the tendency in terms of GNC algorithms is to simplify and reduce the missionization effort to the minimum. This is particularly necessary for European launch systems offering ride-share missions such as the VEGA Small Spacecraft Mission Service (SSMS) [19].

Indeed, the design of such algorithms should reconcile different needs: (1) flexibility by allowing payload (PL) changes or swaps without requiring extra tuning efforts; (2) simple and robust concepts in order to simplify the required validation and verification (V&V); (3) designs guided by a higher level of understanding at system level.

Indeed, last minute changes or payload swaps may have an impact on the global bending modes and therefore may require a re-tuning of the bending filters to guarantee full compliance to both stability and noise attenuation requirements. According to the aforementioned design needs, design solutions such as adaptive notch filters that are hard to validate or adaptive attitude control laws that require the

tuning of additional *spectral dampers* for the bending modes [9] have been discarded.

The approach is to not change VEGA's control architecture [6], but rather to achieve a robust tuning of the controller and *understand* how robust it could be to payload changes. To challenge this goal a high-fidelity linear fractional representation (LFR) of a flexible launch vehicle has been designed.

Indeed, LFRs have been successfully applied in aerospace applications. In [4] it has been shown, by means of flight data, that LFRs robustly allow to predict the flutter envelope on the F-16A/B in Heavy Store configuration. In [8] LFRs have been applied for the design of the controllers of a blended wing body aircraft including both dutch-roll and flexible modes. Finally, in [11] a co-design of a large satellite flexible structure has been carried out by applying LFR modelling and by designing a robust reduced order H_∞ controller to meet pointing and mass requirements. This work paved the way for the development of a specific Satellite Dynamics Toolbox for preliminary design phases [16].

As for launchers, a lot of effort has been put in this direction in the past years [10]. It is needed to mention also [12] where LFRs have been used to carry out structured singular value analysis. Moreover, [15] has actually proven the possibility to carry out structured- H_∞ tuning with an LFR of a launch vehicle.

Given these very promising results, an advanced design tool has been recently developed [20]. This tool also provides further insight and understanding of the underlying fundamental design trade-offs at system level, allowing a robust definition and justification of such system requirements. It includes also the definition of a formal approach for uncertainty quantification and modelling, blending together statistical interpretations, system-level margins and a control-theoretic understanding by using linear fractional representations (LFRs). By defining a generic multichannel design model, all high-level technical specifications for the control system are mathematically formalized, enabling robust optimization and worst case analysis. Specific practical difficulties for an effective industrialization such as the need to smoothly schedule the control laws, controller discretization and the curse of dimensionality have been fully addressed with efficient workarounds.

This article shows how this tool has been used for the design of a high-fidelity LFR of the flexible launch vehicle, enabling the possibility to carry out an availability-aware tuning of the bending filters, extending the design's robustness to last minute changes at mission level, ultimately reducing the chances of having to carry out any recurrent bending filter tuning at all.

To demonstrate the proposed concept, the work has been applied considering VEGA-E as a benchmark (see Fig. 1). This launcher is currently in the development phase and is aiming at capturing the small-satellites market. The launcher will have a three stage configuration, leveraging on the P120C and Z40 motors developed for VEGA-C and a new upper stage called M10, which will use liquid oxygen and liquid methane as propellants.

The paper is organized as follows. In section 2 the process of constructing a high-fidelity LFR [20] is discussed. In particular, in section 2.4 the process of building the LFR of the bending modes, including both the modal eigenfrequencies and shapes from the MC of the launcher Finite Element Model (FEM) is described. In section 3 the general methodology [20] for controller optimization and worst case analysis is introduced. In section 4 worst case analysis with an off-the-shelf bending filter is shown. Moreover, by setting the uncertainties on the payload configuration an availability certificate is computed and justified. Finally, the complicated task of designing availability-aware control laws is solved.

2 HIGH-FIDELITY LFR OF A LAUNCH VEHICLE

In this paper, the linearized launcher equations [7] are not presented for the sake of brevity. The focus is not on the state space model, but on the *generalized* state space model that includes the parametric uncertainties. Previous works [12] [15], feature bending parameter LFRs that have been defined with



Figure 1: VEGA-E Launcher

lump sum system-level margins, ignoring which are the driving parameters that yield uncertainty or variety. In this work, a practical implementation of the proposed new *paradigm* [20] is shown, proving the industrial benefits of a modelling and design technology supported by system-level knowledge. Indeed, the MC analysis discussed in section 2.4 has not been computed to just identify the *ranges* for such parameters, but to *model* the MC within the generalized state space model itself. This is carried out with a methodology [20] that works out just the same for the remaining parameters of the linearized model: the mass, centre of gravity, inertia, thrust, etc. We may summarize this methodology by describing the key steps:

1. The data package shall be standardized; the input scatterings χ_j of the MC shall be independent, time-invariant and defined in the closed interval $[-1, 1]$; in this sense, we may call such scatterings "fundamental scatterings".
2. MC analyses is performed in order to measure each i -th dispersed output parameters p_i needed to characterize the linearized state space model and return such parameters with respect to an appropriate scheduling variable.
3. It is more practical to not model negligible correlations between parameters. Thus, we compute the Pearson Correlation Coefficients (PCC) between the fundamental scatterings and the dispersed output parameters of the MC. By setting a threshold on the PCCs, it is easy to understand which correlations need not to be modelled. This yields for each i -th parameter p_i a subset of meaningful fundamental scatterings A_i .
4. Each parameter is assumed to be correlated by a subset of fundamental scatterings by means of a linear regression model (see the *correlated approach* in [6]). This assumption is deemed reasonable since such dispersions are usually smooth mappings around the nominal values. The linear modelling of the i -th parameter is defined as:

$$p_i = p_{i0} + \frac{\bar{r}_i - \underline{r}_i}{2} + \sum_{j \in A_i} \beta_{ij} \chi_j + \frac{\bar{r}_i + \underline{r}_i}{2} \rho_i \quad (1)$$

Where in Eq. 1, p_{i0} is the mid-range value obtained from MC analysis, \bar{r}_i and \underline{r}_i are respectively the upper and lower bounds of the residual of the linear regression model, β_{ij} is the regression slope and ρ_i is the residual scattering parameter. The model in Eq. 1 is always a balance between two design knobs: the threshold on the PCCs that quantifies how many dependencies

are to be modelled and a threshold on the residuals that avoids having to include residuals when negligible. By lowering the threshold on the PCCs more dependencies are modelled: conservatism is decreased. By lowering the threshold on the residuals, the larger is the total range of p_i : conservatism is increased.

5. The two sets of uncertain parameters $\chi_{j \in A_i}$ and ρ_i form the Δ_i of the LFR of p_i , thus we may consider each parameter to be modelled by:

$$p_i = M_i \star \Delta_i \quad (2)$$

Where in Eq. 2, M_i is the completely nominal part of the LFR and the \star symbol represents the Redheffer star product.

2.1 Trajectory Dispersions

The number of repetitions of a given fundamental scattering in the generalized state space model allows to have a gut-level understanding of a design driver's influence on the complete dynamics. This is especially the case for the fundamental scatterings that affect the launcher secular dynamics when linearizing the system equations.

Take as an example the engine dispersions of a solid rocket motor [6]:

$$T = T_0 (t^*) \frac{(1 + \chi_{m_p})(1 + \chi_{ISP})}{1 + \chi_{tc}} \quad (3)$$

$$\dot{m} = \dot{m}_0 (t^*) \frac{1 + \chi_{m_p}}{1 + \chi_{tc}} \quad (4)$$

$$t^* = \frac{t}{1 + \chi_{tc}} \quad (5)$$

Where χ_{tc} is the combustion time scattering, χ_{ISP} is the specific impulse dispersion, χ_{m_p} is the dispersion on the initial propellant mass, T is the thrust, T_0 is the nominal thrust, \dot{m} is the mass flow, \dot{m}_0 is the nominal mass flow and t^* is the time scheduling dispersion. Indeed, it is particularly interesting to understand how the engine's fundamental scatterings affect the other parameters of the system such as the non-gravitational acceleration \bar{g} , the Mach number (M), thus the aerodynamic center of pressure x_{cp} , aerodynamic normal force coefficient derivative ($c_{n\alpha}$) and aerodynamic axial force coefficient (c_a), just as much as the relative velocity V_{rel} and therefore the dynamic pressure Q . The propagation of all such dependencies is often very complex and at times even interrelated. We may say in this sense that the secular dynamics' *dispersion*, which indeed accounts for an important part of the uncertainty due to linearization, is now embedded in the generalized state space model.

In practice, by following the steps described in section 2, a simplified simulator is used to compute a computationally cheap 3DOF MC analysis [6] that allows to characterize with sufficient precision the trajectory dispersions and therefore the impact of the fundamental scatterings that affect the point-mass dynamics:

1. Propulsive scatterings (see Eq. 3, Eq. 4 and Eq. 5);
2. Mass budget scatterings;
3. Aerodynamic modelling scatterings;
4. Atmospheric modelling uncertainties;

The choice is to consider as scheduling variable the non gravitational velocity (VNG), as this is the scheduling variable of the control law too [6].

Thus, a post-processing is carried out by computing the PCC and effectively neglecting the not meaningful correlations. Finally, Eq. 1 allows to compute the linear regression model of the parameters of the system p_i and therefore define the LFRs.

With this approach [20], conservatism due to trajectory dispersions is dosed in a formal way, without having to support the scattering policy with conjectures around possible worst-cases for specific design requirements or tuning goals.

2.2 Rigid Dynamics

If the MC computed in section 2.1 is carried out on a cheap 3DOF simulator, some work is still needed to extend the analysis to properly model the rotational dynamics.

Firstly, the dispersions on the centre of gravity and moments of inertia need to be computed. This is carried out by firstly computing a MC over the mass, centre of gravity and moments of inertia at system level, considering the "program phase" maturity margins of each item of the mass budget. Secondly, the outcome of the MC is *resampled* considering the dispersions on the mass flow (see Eq. 4). It must be highlighted that since we are aiming with the high-fidelity LFR at defining an availability certificate for the control system, the mass and position of the payloads will certainly be fundamental scatterings *driving* the LFRs of the MCI (mass, center of gravity and moment of inertia). A more complex aspect is the aerodynamics modelling.

Indeed, the trajectory dispersions described in section 2.1 allow to compute the dispersions on the Mach number (M). Thus, by re-sampling the aerodynamic coefficients, the fundamental parameters that affect the (M) may be modelled in the LFRs of the aerodynamic parameters or accounted for in the residuals.

Nevertheless, in general, the aerodynamic parameters x_{cp} and c_n depend also on the Reynolds number (Re), the roll angle φ and the *angle of attack* α .

The dispersed (Re) has not been taken from the dispersed trajectories. Contrary to the (M), the current aerodynamic data package does not allow to look-up its effect upon the aerodynamic parameters. The same consideration is applied for what concerns the effect of φ , that accounts for geometric protrusions that make the launcher not perfectly axially symmetric.

The aerodynamic coefficients are provided as functions of the (M) and α only. Nevertheless, these remaining effects are considered in the total modelling uncertainty of these parameters, provided by an aerodynamic system margin.

The effect of α could be embedded in the LFR by considering it both as a variable α and an uncertain parameter δ_α , to be included in the total Δ of the generalized state space model [3]. This would allow to model the correlation due to α , providing a less conservative modelling of the aerodynamics. Again, this is a more accurate representation of linearization uncertainty enabled by the generalized state space model.

2.3 Sloshing

It is worth to note that dispersed p_i may trigger also other parametric dispersions. For instance, \bar{g} affects the slosh modal frequencies ω_{sj} and damping ratio ζ_{sj} . Indeed, these parameters need to be scaled in order to comply respectively to the Froude number (Fr) and Reynolds number (Re) mechanical similarities.

Of course, the slosh model would anyhow be dispersed also by other fundamental scatterings to consider its intrinsic modelling uncertainty.

2.4 Bending Analysis

In this section, the process of constructing the LFRs of the bending parameters is described. Since the goal of this activity was to essentially prove a concept, the analysis was carried out, without loss of generality, with a simplified finite element model built upon 1D beam elements. A more detailed analysis can be carried out in the future considering a high-fidelity FEM model of the launcher.

The computation of the global bending modes has been carried out with the reduced-body approach for what regards sloshing, yet considering the actuators to be locked [17]. Indeed, the choice of improving the modelling accuracy with the reduced-body approach, implies that the modal analysis has been carried out by removing the slosh masses m_{sj} of the uncertain mechanical equivalent *model* for sloshing. Hence, as a consequence the *slosh modelling uncertainty* impacts also the bending uncertainty to a certain extent.

In a specific mission, the payload configuration is more or less known. Nevertheless, since in this work we are interested in verifying robustness to payload variability, we shall consider a MC spanning all possible PL configurations according to the high-level system specifications.

To construct the LFR, a MC (N=2000) of the FEM model has been computed by scattering:

1. the stiffness EI of each item of the launcher stiffness budget
2. the non-structural inert masses of each stage;
3. the sloshing masses m_{sj} of the Vega upper stage (VUS);
4. the payload properties including the centre of gravity x_{PL} , fundamental lateral bending frequency f_{PL} and mass m_{PL} ;

Thus, the FEM analysis allows to identify the bending eigenfrequencies ω_{bi} and modal shapes ϕ_i . In reality, the flexible launch vehicle model for GNC studies requires only the knowledge of the modal translations ψ_i and rotations σ_i in specific points of application along the launcher centerline: the engine pivot point x_{PVP} , the position of the inertial navigation system x_{INS} and the j-th slosh mass equilibrium points x_{sj} . All such points are also *dispersed* and therefore the dispersed bending parameters of the FEM analysis are *sampled* accordingly over the centerline.

It is highlighted that the FEM analysis does *not* consider engine dispersions on the mass flow \dot{m} , that is affected by the engine *fundamental* scatterings in Eq.4. Nonetheless, these dispersions do have an effect on the bending modes. This is handled by considering the dispersed bending parameters returned from the FEM analysis to be *scheduled* with a nominal mass flow. The dispersed mass flows \dot{m} (see Eq. 4) returned from the MC analysis described in section 2.1, would be propagated by simply *interpolating* the dispersed bending parameters with the measured mass flows of the MC. If the PCC for a given bending parameter p_i is above the user defined threshold, then χ_{mp} and χ_{tc} may explicitly be modelled in the LFR. Otherwise, the effect may be anyhow considered with the bending parameters' ρ_i .

As for the bending frequencies', shift due to thrust [17] is neglected as it is a very small effect on VEGA launchers.

2.5 Actuator Model

An important element for the verification of stability and robustness margins related to bending is provided by the actuator model, as it has an important effect in the frequency range of interest. The reader is referenced to [5] for a detailed 2-DOF modelling of the actuator. To simplify the most possible the size of the model, parameters that are dependent to thrust are left uncorrelated. The small-loop

controller also contributes very much to the size of the model, yet it only contributes to the nominal part of the generalized state space model. To robustly compress this part, a balanced truncation of the nominal part of the actuator subsystem is carried out.

Since the thrust vector control (TVC) is assumed to be "prescribed", the dog-wags-tail effect is neglected, though the effects of nozzle angular rotations on the rigid dynamics (tail-wags-dog effect) is kept.

3 METHOD

This section shortly describes the general method introduced in [20]. Firstly, in order to carry out any sort of dynamic programming with the LFR of the flexible launcher, it is needed to formalize all *high-level* technical specifications as mathematical functions, i.e.: as *low level* requirements. All such *low level* requirements are modelled to be bounds over H_2 or H_∞ norms to be verified with the high-fidelity LFR.

The solver [13], SYSTUNE, is commercially available in Matlab and allows to solve the following dynamic programming problem:

$$\min_x \max_\delta (\alpha \mathbf{f}(x, \delta), \mathbf{g}(x, \delta)) \quad (6)$$

where, in Eq. 6, x is a vector of tunable parameters in the control law that are all defined in given intervals, δ is a vector of uncertain parameters (that make up the Δ of the LFR), f is a low-level objective function, g is a low-level constraint function and α is a multiplier that the solver adjusts in order to force the solution to the original constrained optimization problem.

The subproblem,

$$\max_\delta (\mathbf{f}(\delta)) \quad (7)$$

is what we refer to as worst case (WC) analysis and is verified one requirement $f(\delta)$ at a time.

The high-fidelity LFR of the launcher features a very large Δ (its size is ~ 700). The problems in Eq. 7 and especially Eq. 6 appear to be computationally *not feasible* because of the well-known curse of dimensionality. The technological enabler in this case is given by what Apkarian calls the "dynamic inner approximation" method [13]. As it allows to formally carry out sensitivity analyses for each iteration step, by defining an "active scenario" without lacking overall robustness.

In [20], the setting described in Eq. 6 is used to tune the complete control laws achieving robustness both in terms of stability margins and load relief. In this article we shall focus on the sub-problem that concerns the synthesis of the bending filters, to show the effectiveness of a high-fidelity LFR of the bending modes.

For this sub-problem, the high level requirements to be verified are the following [6]:

1. Low Frequency Delay Margin (LFDM)
2. High Frequency Gain Margin (HFGM)
3. Fundamental Bending Mode Delay Margin (BM1DM)
4. Upper Bending Modes' Gain Attenuation (BMU Att.)

All such requirements need not to be necessarily verified only by analysing the open-loop return difference $L_i = KG$, but can also be verified in closed-loop [1] by analysing the sensitivity function $S_i = (I + L_i)^{-1}$ and complementary sensitivity function $T_i = L_i (I + L_i)^{-1}$. Indeed, this allows to define *templates* [2] that enable a more robust *low-level* verification of stability. In practice, this is

carried out by verifying the tuning in a closed-loop multichannel design model [20] where the S_i and T_i can be taken by selecting specific input and outputs.

The HFGM is the highest real amplification gauge gain that can be added to the input break-point without having the return difference cross the critical point. Therefore the HFGM is verified by complying to:

$$f_{GM} = |T_i|_{\infty} \leq \frac{1}{GM - 1} \quad (8)$$

$$g_{GM} = |S_i|_{\infty} \leq \frac{GM}{GM - 1} \quad (9)$$

Where in Eq. 8, $|T|_{\infty}$ is considered as the objective function instead of $|S|_{\infty}$ essentially because the complementary sensitivity function is more "sensible" and may add non-necessary conservatism to the optimization problem.

The LFDM is the highest delay that can be added to the input break-point without having the return difference cross the critical point at a frequency lower than that of the first bending mode. Whereas the BM1DM is conceptually the same, but verified around the first bending mode frequency. Both DMs are verified formally by complying to:

$$|S_i|_{\infty} \leq \frac{1}{2 \sin \frac{PM}{2}} \quad (10)$$

$$|T_i|_{\infty} \leq \frac{1}{2 \sin \frac{PM}{2}} \quad (11)$$

Contrary to Eq. 9 and Eq. 8, the delay margin requirement is frequency-dependent, because

$$PM = \frac{180}{\pi} DM \omega \quad (12)$$

In general, the sensitivity function S is more "sensible" at the lower frequencies, whereas the complementary sensitivity function T at the higher frequencies. While for the HFGM we already know which function is most severe; for the LFDM this is not the case. This very much depends on the perturbations that may affect the system and the design of the control laws. As for the BM1DM, the low-level requirement on the sensitivity function is more sensitive in the "half-plane" of the Nichols chart in which open-loop gain is negative, whereas the complementary sensitivity function is more sensitive where the open-loop gain is positive. This implies that by setting the complementary sensitivity function as a constraint the optimization will not attempt to gain control the bending mode, while it shall optimize the sensitivity function to phase-control by design.

The BMU Att. requirement is essentially a margin on the passive stabilization of the upper bending modes. The desired attenuation gain L_u on the return difference L_i is verified by complying to:

$$g_{BMU} = |T_i| \leq \left| \frac{L_u}{1 + L_u} \right| \quad (13)$$

It is worth mentioning that the low-level requirement in Eq. 13 is more conservative than the high-level requirement on the return difference matrix, $|L_i|_{\infty} < L_u$, as it adds more severity around the critical point providing additional robustness to the controller.

It may be noticed that the approach [20] is to consider verifying stability requirements both with the S_i and the T_i . Alternatively, the designer could choose to verify margins with the *disk* margin policy that effectively mixes the two sensitivities by tuning the skew parameter [18].

Nevertheless, the disk margin is defined as the largest complex multiplicative factor that makes the L_i cross the critical point, which in general accounts for a mixed gain-phase perturbation. Compared

to classic evaluations of gain and phase margins, the disk margin offers the advantage of being more robust, since a small combined perturbation could quickly degrade the pure gain and phase margins. Yet by verifying the stability margins with the S_i and T_i this is also prevented. The choice is to disregard disk margins because it is less easy to *reconstruct* from a disk margin low-level requirement a high-level system requirement on the gain and phase margins. In an industrial context, it is very important to not loose a direct connection with the classic high-level requirements that are understood by non-specialist system engineers. Moreover it is also useful from a system engineering point of view to understand which perturbations degrade stability both from a *dominantly* gain and phase point of view, rather than the combined effect.

4 APPLICATIONS

As it has been mentioned, the work in this article has been carried out considering VEGA-E as a study case. In this regard, it was believed [14] that for future European launchers the tuning and verification of the bending filters, meeting the BM1DM and the BMU Att. requirements, was necessarily a mission-dependent activity.

On the contrary, this work proves that the high-fidelity LFR discussed in section 2 enables the designer to formally define an *availability certificate* that allows to *measure* to what extent a given tuning may be considered applicable to different payload configurations. Such metric can also be used to optimize the control tuning in order to increase the availability metric making the controller tuning more generic and therefore overcome the mission-dependency of the controller. This example shows how *effective* is the LFR-based paradigm [20] compared to designs carried out with "corner case" multi-models or pre-defined worst case models. The difference is essentially in the additional system level understanding, that other methods can't provide. Moreover, a formal verification of the worst cases by means of LFRs prevents the designer from *not* recognizing changes in the worst case perturbations that are triggered by changes in the controller tuning. Such tool [20] allows the designer to introduce improvements in the control laws with a much higher level of confidence, without fearing the consequences of finding unexpected behaviors in the final verification and validation phase.

4.1 Worst Case Analysis

The general approach [20] is to consider the same *low-level* requirements for both the *tuning* and *verification* of the system requirements. This is what effectively allows the designer to trust the methodology making it a design *paradigm*.

As an example, we have solved Eq. 7 by applying the high-fidelity LFR described in section 2 on a previous tuning tailored to a specific max payload configuration. Results are reported in Table.1 as weighted requirements: any requirement previously described as $|S_i|_\infty \leq W$ or $|T_i|_\infty \leq W$ becomes respectively $|W^{-1}S_i|_\infty \leq 1$ or $|W^{-1}T_i|_\infty \leq 1$.

Table 1: Worst Case norms for a tuning tailored to a max payload configuration

Channel	Requirements			
	LFDM	HFGM	BM1DM	BMU Att.
T_i	0.64	0.84	1.77	0.76
S_i	0.80	0.76	0.84	-

It can be clearly seen that this controller is not compliant to the BM1DM requirement. This was expected, because the payload mass adds a shift to the first bending mode frequency, compromising

its active stabilization. Indeed, by solving Eq. 7 we also obtain the worst case perturbation for each requirement (see Figure 2), a precious outcome of the analysis that adds a layer to the system-level understanding in the design trade-offs.

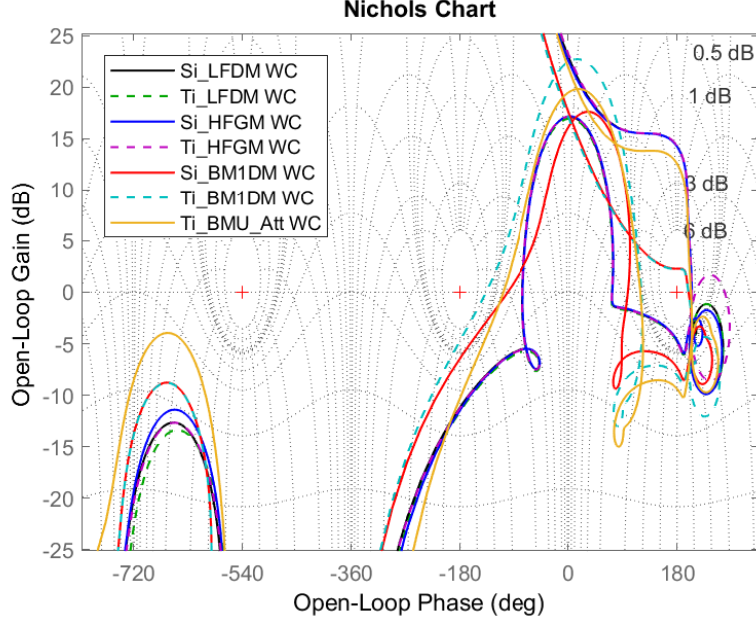


Figure 2: Worst Case Analysis

4.2 Availability Certificate

The high-fidelity LFR of the launcher described in section 2 explicitly features the payload mass $\chi_{m_{PL}}$ and the centre of gravity $\chi_{x_{PL}}$, whereas the effect of the payload lateral frequency f_{PL} was not found to be worthy of being modelled (its PCC is below the threshold). For the verification of the BM1DM and BMU Att. requirements the driver is definitely the $\chi_{m_{PL}}$, thus we can define the *availability certificate* problem as follows:

$$AV = \max_I \max_{\delta} f(\delta, I) \quad (14)$$

Where $\chi_{m_{PL}} \in I = [\mu_l, \mu_u]$. The dependency of f to I is given by the fact that the BM1DM and BMU Att. requirements are verified in frequency ranges that effectively depend on I . The problem in Eq. 14 is only apparently much more complicated than that defined in Eq. 7. It can be solved by firstly considering the largest interval $[-1, 1]$ and solving Eq. 7 by computing the worst case δ : this is obviously more conservative, but such extra conservatism in the computation of AV can be removed by carrying out a simple post-processing on the result. If $AV = [-1, 1]$, the availability certificate states that the controller can fly any possible payload configuration considered at system level. If by solving Eq. 7 it appears that $AV \subset [-1, 1]$, the effective I needs to be refined. This can be carried out by progressively reducing the μ_l and μ_u from -1 and 1 to 0 until all weighted requirements f are fulfilled. In this post-processing, the worst case δ is anyhow fixed except for $\chi_{m_{PL}}$, as it is only a matter of finding the critical range for $\chi_{m_{PL}}$.

Take as example the mission-specific tuning analyzed in section 4.1. In this case, $AV = (0.6, 1]$, which can be easily mapped back to the system-level interval, $[\underline{m}_{PL}, \overline{m}_{PL}]$. In Fig.3, a Nichols chart

showing the worst case perturbation on the BM1DM is included, comparing the worst case perturbation obtained by solving Eq. 7 with that obtained by computing the availability certificate in Eq. 14. For very tight design problems, an availability *certificate* can be considered by mission managers to understand the impact of last-minute payload configurations at a controllability level, without having to perform any assessment both in terms of FEM modal analysis and control system tuning.

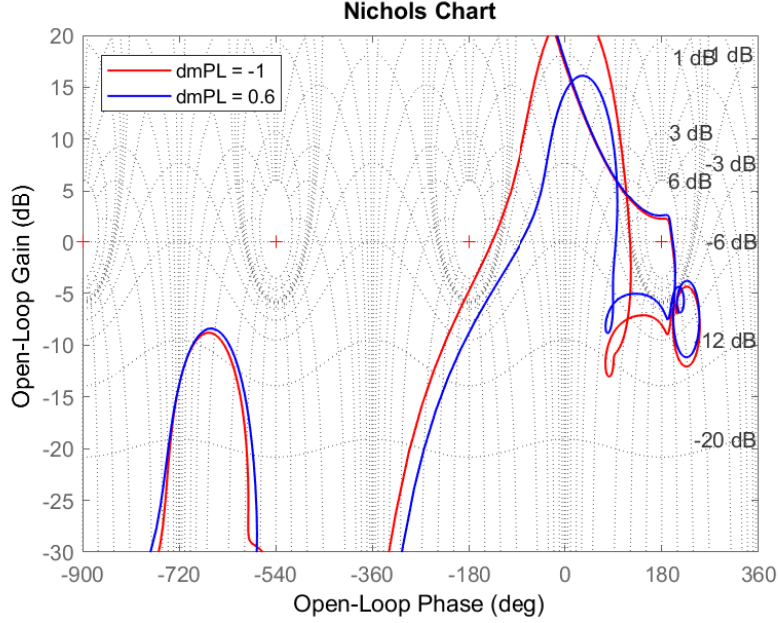


Figure 3: A Nichols Chart Showing the AV

4.3 Generic Control Law Tuning

Now we want to optimize x in the attempt of having AV reach $[-1, 1]$, or in other words we seek to achieve a bending filter that is fully generic.

For this scope, we may compute Eq. 6 to optimize the bending filter H_3 in the controller architecture [6]:

$$H_3(p) = \prod_{i=1}^N \frac{\frac{p^2}{\omega_{Ai}^2} + 2\frac{\eta_{Ai}}{\omega_{Ai}}p + 1}{\frac{p^2}{\omega_{Bi}^2} + 2\frac{\eta_{Bi}}{\omega_{Bi}}p + 1} \quad (15)$$

Where p is the Heaviside derivative operator.

By completing this task, all low-level requirements are met (see Table 2). It can be seen that the BM1DM has been made compliant but at the expense of a better trade-off with the HFGM requirement. Yet, in this case, $AV = [-1, 1]$, thus the new H_3 filter is effectively generic.

Table 2: Worst Case norms after tuning with the proposed high-fidelity LFR

Channel	Requirements			
	LFDM	HFGM	BM1DM	BMU Att.
T_i	0.73	1.00	1.00	0.59
S_i	0.88	0.85	0.64	-

The worst case perturbations for the generic tuning are shown in Figure 4.

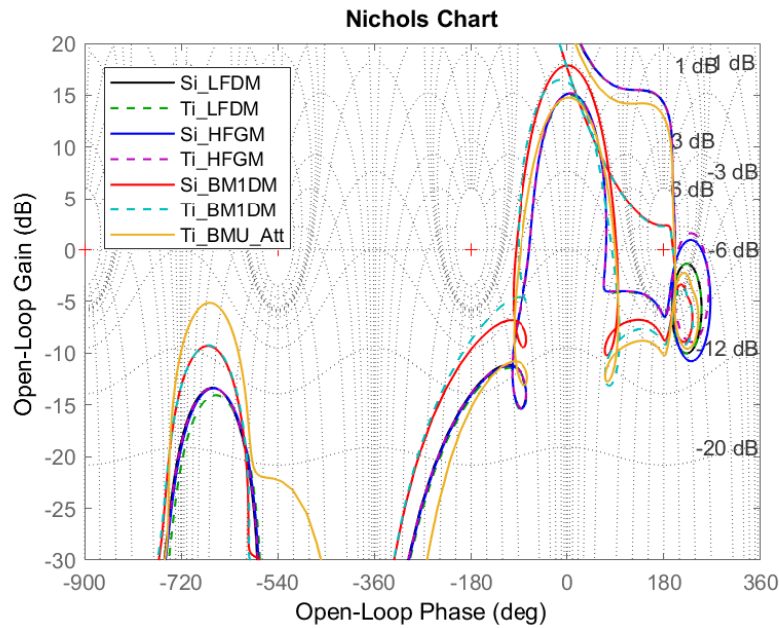


Figure 4: Worst Case Analysis with Generic Tuning

5 CONCLUSIONS

A new robust control *paradigm* [20] has been applied to define high-fidelity generalized state space models for a flexible launch vehicle, allowing to provide to the mission management an *availability* certificate on the control law that measures robustness to last minute changes in the payload configuration. The generalized state space model enables also the possibility to robustly tune the controller making it more generic.

The approach has been applied on a highly detailed design model, taking VEGA-E as a benchmark, proving that the new *paradigm* can be industrialized on European launchers.

ACKNOWLEDGEMENTS

We are deeply grateful to Samir Bennani and Pedro Simplicio for their important support in the design and follow-up of the advanced design tool [20] in the frame of esa contract no.4000124574/18/nl/crs.

REFERENCES

- [1] M. G. Safonov, A. J. Laub, and G. Hartmann, “Feedback properties of multivariable systems: The role and use of the return difference matrix,” *IEEE Transactions on Automatic Control*, vol. 26, 1981.
- [2] I. Horowitz, “Quantitative feedback theory,” in *IEE Proceedings D (Control Theory and Applications)*, IET, vol. 129, 1982, pp. 215–226.
- [3] D. Farret, G. Duc, and J. Harcaut, “Discrete-time lpv controller for robust missile autopilot design,” *IFAC Proceedings Volumes*, vol. 35, no. 1, pp. 127–132, 2002.
- [4] S. Bennani, B. Beuker, J. W. Van Staveren, and J. J. Meijer, “Flutter analysis of an f-16a/b in heavy store configuration,” *Journal of aircraft*, vol. 42, no. 6, pp. 1565–1574, 2005.

- [5] C. Renault, “Usefulness of a force feedback on electromechanical actuator,” in *Guidance, Navigation and Control Systems*, vol. 606, 2006.
- [6] C. Roux and I. Cruciani, “Scheduling schemes and control law robustness in atmospheric flight of vega launcher,” in *Proceedings of the 7th ESA International Conference on Spacecraft Guidance, Navigation and Control Systems*, 2008, pp. 1–5.
- [7] J. Orr, M. Johnson, J. Wetherbee, and J. McDuffie, “State space implementation of linear perturbation dynamics equations for flexible launch vehicles,” in *AIAA Guidance, Navigation, and Control Conference*, 2009, p. 5962.
- [8] A. Schirrer, C. Westermayer, M. Hemedi, and M. Kozek, “Robust lateral blended-wing-body aircraft feedback control design using a parameterized lfr model and dgk-iteration,” *Progress in flight dynamics, guidance, navigation, control, fault detection, and avionics*, vol. 6, pp. 749–766, 2013.
- [9] J. H. Wall, J. S. Orr, and T. S. VanZwieten, “Space launch system implementation of adaptive augmenting control,” in *Annual American Astronautical Society (AAS) Guidance, Navigation, and Control Conference*, 2014.
- [10] A. Marcos, S. Bennani, C. Roux, and M. Valli, “Lpv modeling and lft uncertainty identification for robust analysis: Application to the vega launcher during atmospheric phase,” *IFAC-PapersOnLine*, vol. 48, no. 26, pp. 115–120, 2015.
- [11] H. H. S. Murali, D. Alazard, L. Massotti, F. Ankersen, and C. Toglia, “Mechanical-attitude controller co-design of large flexible space structures,” in *Advances in Aerospace Guidance, Navigation and Control: Selected Papers of the Third CEAS Specialist Conference on Guidance, Navigation and Control held in Toulouse*, Springer, 2015, pp. 659–678.
- [12] P. Simplicio, S. Bennani, A. Marcos, C. Roux, and X. Lefort, “Structured singular-value analysis of the vega launcher in atmospheric flight,” *Journal of Guidance, Control, and Dynamics*, vol. 39, no. 6, pp. 1342–1355, 2016.
- [13] P. Apkarian and D. Noll, “The H_∞ Control Problem is Solved,” *Aerospace Lab*, no. 13, pages 1–11, Nov. 2017.
- [14] M. Ganet-Schoeller, J. Desmariaux, and C. Combier, “Structured control for future european launchers,” *Aerospace Lab*, no. 13, pages–1, 2017.
- [15] D. Navarro-Tapia, A. Marcos, P. Simplicio, S. Bennani, and C. Roux, “Legacy recovery and robust augmentation structured design for the vega launcher,” *International Journal of Robust and Nonlinear Control*, vol. 29, no. 11, pp. 3363–3388, 2019.
- [16] D. Alazard and F. Sanfedino, “Satellite dynamics toolbox for preliminary design phase,” in *43rd Annual AAS Guidance and Control Conference*, vol. 30, 2020, pp. 1461–1472.
- [17] T. M. Barrows and J. S. Orr, *Dynamics and Simulation of Flexible Rockets*. Academic Press, 2020.
- [18] P. Seiler, A. Packard, and P. Gahinet, “An introduction to disk margins [lecture notes],” *IEEE Control Systems Magazine*, vol. 40, no. 5, pp. 78–95, 2020.
- [19] C. Roux, E. Nardi, and N. Romanelli, “Vv16: The first vega rideshare mission: Lessons learnt after successful flight,” 2021.
- [20] M. Aveta, “Adaptive flight guidance and control systems with reconfiguration, [final report], esa contract no.4000124574/18/nl/crs,” 2023.